



## Study of Laser Propagation Parameters in the Underdense Plasma Region Using a Two Dimensional Simulation Code

A. Hadi Al-Janabi      Mazin M. Elias      and      M. Sh. Mahmood

*Institute of Laser and Plasma for Postgraduate Studies, University of Baghdad,  
P.O. Box 47314 Jadiriah, Baghdad, IRAQ    e-mail: [plasma@uruklink.net](mailto:plasma@uruklink.net)*

(Received 8 June 2002; accepted 8 October 2002)

**Abstract:** The propagation of laser beam in the underdense deuterium plasma has been studied via computer simulation using the fluid model. An appropriate computer code “HEATER” has been modified and is used for this purpose. The propagation is taken to be in a cylindrical symmetric medium. Different laser wavelengths ( $\lambda_1 = 10.6 \mu\text{m}$ ,  $\lambda_2 = 1.06 \mu\text{m}$ , and  $\lambda_3 = 0.53 \mu\text{m}$ ) with a Gaussian pulse type and 15 ns pulse widths have been considered. Absorption energy and laser flux have been calculated for different plasma and laser parameters. The absorbed laser energy showed maximum for  $\lambda = 0.53 \mu\text{m}$ . This high absorbitivity was inferred to the effect of the pondermotive force.

### Introduction

The study of laser – produced plasma is one of the fastest growing fields of present – day applications [1]. A rich variety of collective processes can play an important role in the coupling, particularly in the very large regions of underdense plasma [2]. During the interaction of a high power laser beam with a target, many processes will arise. Laser beam might absorbed, reflected or propagated through the formed plasma. A rich variety of coupling processes as a function of the plasma density have been observed [3]. Near the critical density ( $n_{cr}$ ), there are resonance absorption and instabilities leading to the excitation of electron and ion waves. Near  $n_{cr} /4$ , there is the  $2w_{pe}$  instability.

For densities less or equal  $n_{cr} /4$ , Raman instability is operating, and throughout the underdense (as does inverse bremsstrahlung absorption), the Brillouin and filamentation instabilities take place. Throughout the underdense plasma, there can be self – generated magnetic fields of ion turbulence driven by a

variety of processes associated with the plasma heating and expansion [3]. Different approaches have been adopted to study the aforementioned coupling processes and the laser propagation parameters in underdense plasma region [1,4-7]. A computer simulation using different models has been conducted to study the laser propagation and coupling with plasmas [8-10].

The motivation of the present work is to study the laser beam propagating in a cylindrical shape inside the plasma region using a modified version of a computer code “HEATER”. The absorption energy and laser fluxes have been calculated for different plasma and laser parameters.

### Basic Theory

Simulation is the process of designing a model of a real system and conducting experiments with this model for the purpose, either of understanding the behavior of the system, or of evaluating various strategies (within the limits imposed by criterion or set of criteria) for the

operation of the system [11]. Simulation is a very active tool in studying plasma behavior. Plasma simulation codes have widely been used to a certain extent as an alternative for the costly plasma experiments. One of these codes, which were used in the present work, is the "HEATER" program [13].

This simulation illustrates the inclusion of self-generated magnetic field; its influence on

transports properties and consequent an isotropic behavior [2].

"HEATER" was designed to replace the laser package of the 2D target code, "CASTOR 2", which ignores diffraction and refraction and does not calculate the radial ponderomotive force [12].

For a laser of angular frequency ( $\omega$ ) in a medium with dielectric constant  $\epsilon(r)$ , the transverse electric field amplitude ( $E$ ) satisfies the Helmholtz equation

$$\nabla^2 E + \frac{\omega^2}{C^2} \epsilon(r) E(r) = 0 \dots\dots (1)$$

If the medium is a plasma with electron collision frequency ( $\nu_c$ ),  $\epsilon(r)$  is approximately given by [13]:

$$\epsilon(r) = 1 - \frac{\omega_p^2}{\omega^2} (1 - i\nu_c/\omega) \dots\dots (2)$$

By considering a laser propagating in the positive z-direction along the axis of a cylindrically symmetric plasma, the fast phase variation of  $E$  may be separated out by defining:

$$E(r, z) = \left[ \frac{8pw}{K(z)C^2} \right]^{\frac{1}{2}} f(r, z) \exp\left[ i \int_0^z K(z) dz \right] \dots\dots (3)$$

where:

$$K(z) = \frac{\omega}{C} [\text{Re } \epsilon(o, z)]^{\frac{1}{2}} = \frac{\omega}{C} \left[ 1 - \frac{\omega_p^2(o, z)}{\omega^2} \right]^{\frac{1}{2}} \dots\dots (4)$$

The complex function  $f(r, z)$  is a convenient quantity to work with since it is related to the time-averaged electromagnetic flux ( $F$ ) by :

$$F = |f(r, z)|^2 \dots\dots (5)$$

In the following,  $f$  shall be referred to as the complex flux amplitude. Assuming that variations in  $f$ ,  $\omega_p$  and  $\nu_c$  over one wavelength are small, the equation for the complex flux amplitude is found to be:

$$\frac{\partial f}{\partial z} = \frac{i}{2k} \left[ \frac{1}{r} \frac{\partial}{\partial r} \right] \left( r \frac{\partial f}{\partial r} \right) - q^2(r, z) f(r, z) \dots\dots (6)$$

where

$$q^2(r, z) = \frac{1}{C^2} \{ [\omega_p^2(r, z) - \omega_p^2(o, z)] - i\omega_p^2(r, z)\nu_c(r, z)/\omega^2 \} \dots\dots (7)$$

Introducing the spatial absorption coefficient,  $[K_{abs}(r,z)]$ , so that  $q^2(r,z)$  may be written as :

$$q^2(r,z) = \frac{1}{c^2} [w_p^2(r,z) - w_p^2(o,z)] - ik(z)K_{abs}(r,z).....(8)$$

The absorption coefficient used in “HEATER” is the inverse bremsstrahlung coefficient

$$K_{abs} = 13.51 z \log \Lambda xNe / [I^2 (1 - N_e(N_c))^{1/2} T_e^{3/2}] .....(9)$$

where the Coulomb logarithm is given by Johnston and Dawson [18].

In Eq. (6), the first term on the right side causes diffraction of the beam and the second term causes refraction and absorption. The power absorbed per unit volume is [20]

$$W_{las} = K_{abs}(r,z) |f(r,z)|^2 .....(10)$$

The axial and radial ponderomotive forces are

$$f_z(r,z) = -\frac{w_p^2(r,z)}{2w^2} \frac{\partial}{\partial z} \left[ \frac{|f|^2}{v_g(z)} \right] .....(11)$$

and

$$f_r(r,z) = -\frac{w_p^2(r,z)}{2w^2} \frac{\partial}{\partial r} \left[ \frac{|f|^2}{u_g(z)} \right] .....(12)$$

where  $v_g(z) = K_{(z)} C^2 / W$  is the group velocity of the electromagnetic waves.

## Results and Discussion

The simulation is carried out in cylindrical (r, z) geometry. An arbitrary small temperature was assumed for the initial plasma with an electron density  $N_{e0} = 9.192 \times 10^{23} \text{ m}^{-3}$  with an electron density scale length  $A = 450 \text{ }\mu\text{m}$ , and absorption coefficient  $K_{abs} = 500 \text{ m}^{-1}$ , the beam radius  $R_{max} = 225 \text{ }\mu\text{m}$  and the length of the beam  $Z_{max} = 1500 \text{ }\mu\text{m}$ .

The radial and axial meshes (NR and NZ) are 10 and 40. The laser pulse is triangular with a maximum power of  $10^8$  at 15 ns and falling to zero at 35 ns [14]. The beam focuses at  $Z=0$  to a spot size of 40  $\mu\text{m}$ .

Laser- plasma interaction which has been studied in the present work involves the interaction of three types of lasers ( $\text{CO}_2$ ;  $\lambda_1 = 10.6 \text{ }\mu\text{m}$ , Nd;  $\lambda_2 = 1.06 \text{ }\mu\text{m}$  and second harmonic Nd;  $\lambda_3 = 0.53 \text{ }\mu\text{m}$ ) with plasma. Deuterium

plasma is considered in this interaction. The pulse time is 15 ns. The behavior of the plasma is investigated in the underdense plasma region. Two parameters have been calculated throughout the present work; the laser flux and the absorbed energy.

### The Absorbed Laser Energy Calculations

Figures 1, 2 and 3 illustrate the absorbed laser energy for  $\lambda = 10.6, 1.06$  and  $0.53 \text{ }\mu\text{m}$  respectively. Absorption of the laser radiation is done mostly by inverse bremsstrahlung in which an electron in binary collision with an ion absorbs a photon [15].

Since the plasma frequency scales as density,  $\omega_p \sim n_e^{1/2}$ , it is apparent that laser light incident from the lower density (underdense) region can only propagate up to the density at which  $\omega_p$

becomes equal to  $\omega$  [16]. This limit is usually referred to the critical density.

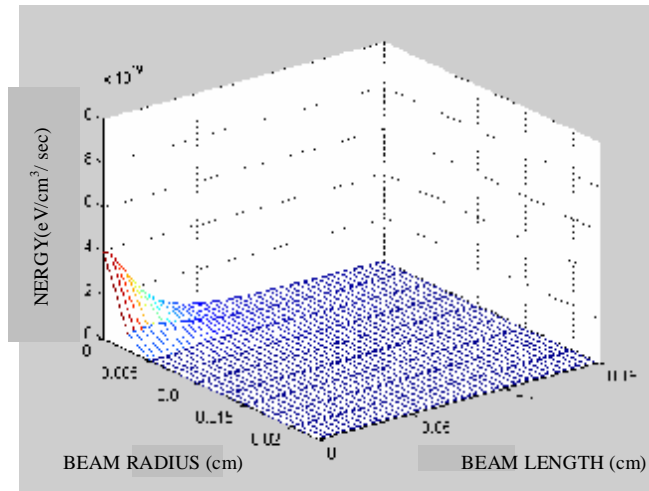


**Fig. 1:** The absorbed energy at  $\lambda = 10.6 \mu\text{m}$

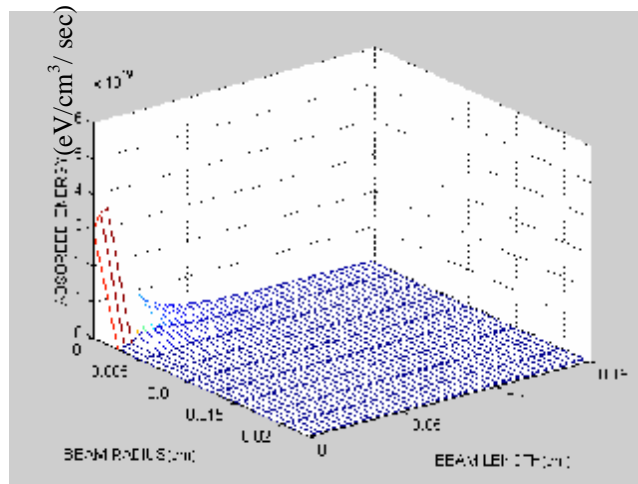


**Fig. 2:** The absorbed energy at  $\lambda = 1.06 \mu\text{m}$ .

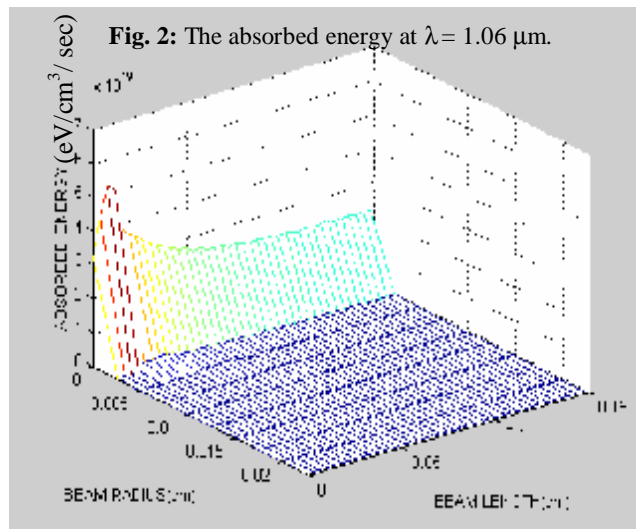


**Fig. 3:** The absorbed energy at  $\lambda = 0.53 \mu\text{m}$ .

At the beginning of the inverse bremsstrahlung process when  $\omega_0 \gg \omega_{pe}$ , the absorbed energy causes an increase in the kinetic energy of the electrons, and this in turn produces further ionization with a subsequent increase in the electron density, so that the electron density increases further and approaches  $n_{cr}$  as shown in Fig. 1 (for CO<sub>2</sub> laser,  $\lambda = 10.6 \mu\text{m}$ ) where the maximum absorbed energy reaches  $4 \times 10^{19}$  eV. At this stage the critical density is established across a plane surface some distance in to the plasma at this point. The plasma becomes opaque to the incoming radiation at which the laser light is therefore reflected out again. When the plasma becomes opaque, laser radiation can no longer reach the surface of the target to generate new plasma by evaporation and ionization [17], so that the absorbed energy decreases until reaching the minimum value at  $Z = 600 \mu\text{m}$  (Fig. 1).

For neodymium laser (1.06  $\mu\text{m}$ ), the maximum amount of energy absorbed is  $3.6 \times 10^{19}$  eV and then decreases rapidly along the z-direction as shown in Fig. 2.

For shorter wavelength lasers, such as the second harmonic of Nd laser with  $\lambda = 0.53 \mu\text{m}$ , the absorption of the energy of this laser is shown in Fig. 3.

The ponderomotive force is very effective in the absorption of the laser energy by the plasma. The values for the both radial and axial ponderomotive forces have been calculated. The radial ponderomotive force is more important than the axial one because it plays an important role in the evaluation of the plasma density profile [14].

For longer wavelength lasers ( $\lambda = 10.6 \mu\text{m}$ ) the maximum amount of the ponderomotive force at the beginning of the laser pulse is  $2.45 \times 10^{11}$  N/m<sup>3</sup>. This force of the beam acts mainly on the region of critical density ( $n = n_{cr}$ ), pushes the plasma back and causes profile modification. After that, the amount of this force decreases along the plasma cylinder because of the increase in the plasma density. In this stage, the laser beam cannot reach the target effectively because of the dense plasma formed above the region. Then the plasma will expand out of the target, the laser beam can reach again the target and the radial ponderomotive force will again rises.

By decreasing the wavelength of the laser beam being used to 1.06  $\mu\text{m}$ , the amount of the calculated pressure is  $3.5 \times 10^9$  N/m<sup>3</sup>. The amount

of the pressure at  $\lambda = 0.53 \mu\text{m}$  is about  $0.9 \times 10^9$  N/m<sup>3</sup> in opposite direction and the ponderomotive force will decrease along the plasma beam. The effect of the radial ponderomotive force is very clear in controlling the absorbed laser energy by the plasma.

### The Laser Flux Calculations

Figures 4, 5 and 6 illustrate the laser flux at  $\lambda = 10.6, 1.06$  and  $0.53 \mu\text{m}$  respectively. The laser irradiance which can be assimilated by thermal conduction in the boundary of the plasma depends on the wavelength of the laser light and on the electron temperature [18].

When the laser wavelength interacted with the plasma is 10.6  $\mu\text{m}$  (CO<sub>2</sub> laser), the maximum laser flux will reach to  $1 \times 10^{17}$  W/cm<sup>2</sup> at  $z = 0$  and decreasing to the minimum amount at  $z = 600 \mu\text{m}$ . That is because there is a reflection of the laser beam from the formed plasma, so that the laser power will be decreased and this will lead to decrease the laser flux as shown in Fig. 4.

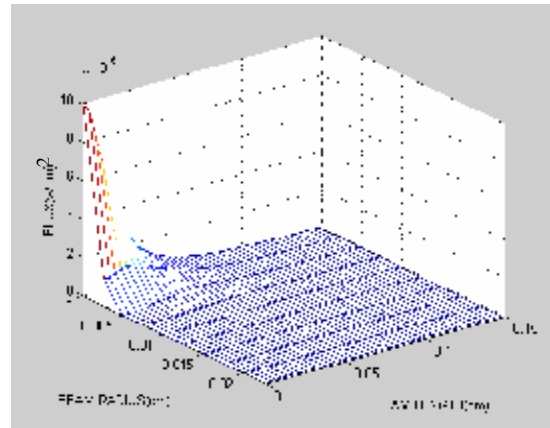


Fig. 4: The laser flux at  $\lambda = 10.6 \mu\text{m}$

Fig. 5 represents the laser flux at  $\lambda = 1.06 \mu\text{m}$ , which reaches to  $1 \times 10^{19}$  W/cm<sup>2</sup> at  $z = 0$  and decreases to the minimum amount at  $z = 200 \mu\text{m}$ . The decreasing of the laser wavelength to 0.53  $\mu\text{m}$  will increase the laser flux to reach to  $4 \times 10^{19}$  W/cm<sup>2</sup> at  $z = 0 \mu\text{m}$  (Fig. 6), and then decreases to about  $1.4 \times 10^{19}$  W/cm<sup>2</sup> at  $z = 100 \mu\text{m}$  and along the plasma cylinder. This

is related to the energy absorption and the ponderomotive force.

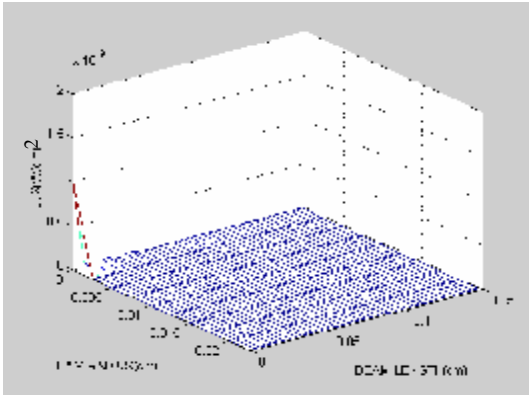


Fig. 5: The laser flux at  $\lambda= 1.06 \mu\text{m}$

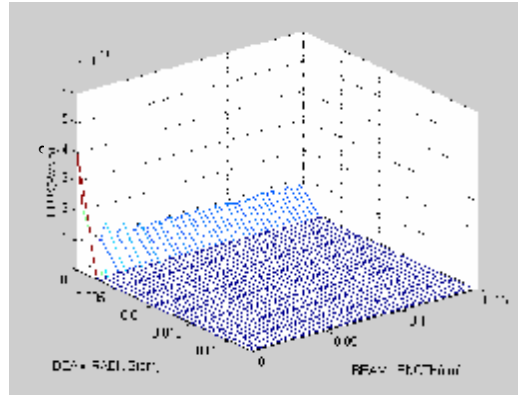


Fig. 6: The laser flux at  $\lambda =0.53 \mu\text{m}$

### Conclusion

The study of the propagation of the laser beam in the underdense plasma region reveals that the absorption of the laser light is done mainly by the “inverse bremsstrahlung” process, which is a binary process.

The absorbed energy by the plasma increases by decreasing the laser wavelength being used. Also, the laser flux increases by decreasing the laser wavelength. The maximum absorbed energy occurs with the second harmonic generation of Nd laser ( $0.53 \mu\text{m}$ ). This might be attributed to the effect of the ponderomotive force. The present study reflects the importance investigating this non-linear process. To avoid the self-focusing inside the plasma, the amount of the ponderomotive force should be calculated during the propagation of the laser beam inside the plasma.

### References

1. L. Wang “Regional College on Plasma Physics”, January (2001) p. 3.
2. R.A. Cairns “Laser – plasma Interaction” Vol II, Scottish universities summer school in physics pub. (1982).
3. W. L. Kruer, “The Physics of Laser–Plasma Interaction”, Addison–Wesley Pub. (1988).
4. W. I. Linlor, *Phys. Rev. Lett.* **12**, 210 (1963).
5. N. S. Yoon, *Phys. Rev. E* **24**, 757 (1996).
6. C. Yamanaka, *Laser and Particle Beams* **8**, 3 (1990).
7. R. J. Jensen, *Fusion Technology* **II**, 481 (1987).
8. C. K. Birdsall and A. B. Langdon “Plasma Physics Via Computer Simulation”, Adam Hilger, IOP Publishing Lib. (1991).
9. T. R. Turner, *Phys. Rev. Lett.* **71**, 1842 (1993).
10. D. I. Choi and N. S. Yoon, *J. Plasma Phys.* **5**, 751 (1998).
11. R. E. Shanon “System Simulation: The Art and Science”, Prentice – Hall, Englewood Cliffs . N.J. (1975).
12. K. V. Roberts, *Comp. Phys. Commun.* **7**, 237 (1974).
13. J. P. Christiansen and N. K. Winsor, *Comp. Phys. Commun.* **17**, 597 (1979).
14. W. L. Kruer, “In Laser– Plasma Interactions”, Sussp. Pub. Edinburgh (1980).

15. J. J. Duderstadt and G. A. Moses, "Inertial Confinement Fusion" John Wiley and Sons, N.Y. (1982).
16. R. J. Bickerton, *Nuclear Fusion* **13**, 457 (1973).
17. H. Saltzman, *Phys. Lett.* **41 A**, 363 (1972).
18. T. W. Johnston and J. M. Dawson, *Phys. Fluids* **16**, 38 (1973).
19. F. F. Chen, "Introduction to Plasma Physics and Controlled Fusion", Plenum Press, N.Y. (1984).
20. J. N. McMullin, C. E. Capjack and C. R. James, *Comp. Phys. Comm.* **23**, 31 (1981).

## دراسة أعلومات سريان حزمة الليزر في البلازما واطئة الكثافة باستخدام برنامج محاكاة ذي بعدين

عبد الهادي مطشر الجنابي      مازن مانويل الياس      محمود شاكر محمود

معهد الليزر والبلازما للدراسات العليا ، جامعة بغداد ، ص. ب 47314 جادرية ، بغداد ، العراق

**الخلاصة** في البحث الحالي تم إجراء عملية المحاكاة بواسطة الحاسوب لبرنامج " HEATER " والذي يمثل دراسة سريان حزمة الليزر في البلازما المتولدة نتيجة تسليط الليزر على هدف مصنوع من الديوتيريوم الصلب باستخدام نموذج المائع. يكون سريان الليزر بشكل أسطواني وتأخذ نبضة الليزر شكل الجرس. تم استعمال أطوال موجية مختلفة في هذا البرنامج هي 10.6 و 1.06 و 0.53 مايكرومتر مع نبضة جرسية الشكل و عرض النبضة هو 15 نانوثانية . يتضمن برنامج HEATER دراسة البلازما المتولدة ببعدين (قطري و محوري ) حيث تكون البلازما بشكل أسطواني باستعمال طريقة التحليل العددي Cubic Spline لحل معادلة السريان لليزر. إن البلازما المتولدة تكون ضمن منطقة الكثافة الواطنة (دون الحرجة) . من خلال تشغيل البرنامج تم حساب كل من الطاقة الممتصة وفيض الليزر وقد لوحظ إن أكبر امتصاص للطاقة يحدث عندما يكون الطول الموجي لليزر 3.5 مايكرومتر والذي يعزى إلى وجود القوة الكابسة .